GRADIENT DYNAMICS

NACA0012 - Gradient Dynamics Solver Validation Study



Gradient Dynamics Ltd.

July 2026

gradient-dynamics.com

contact@gradient-dynamics.com

1. Introduction

The NACA 0012 airfoil is a standard benchmark for validating Reynolds-averaged Navier–Stokes (RANS) solvers and turbulence models. Its simple geometry and extensive experimental and numerical datasets allow predictions of aerodynamic forces, surface pressure and skin friction to be assessed under both attached and high-incidence flow conditions.

This study assesses the Gradient Dynamics FluxCore solver using the standard Spalart–Allmaras (SA) turbulence model. The case follows the NASA Turbulence Modeling Resource (TMR) benchmark. The compressible RANS equations are solved at a freestream Mach number of 0.15 and a chord Reynolds number of 6,000,000:

Simulations are performed at angles of attack of 0°, 10° and 15°. Predicted lift, drag, surface-pressure coefficient and skin-friction coefficient are compared with available experimental measurements and established CFD reference data. The NASA Family II, Level-4 grid is used because the aerodynamic coefficients and grid-convergence behaviour are sensitive to the streamwise resolution near the sharp trailing edge.

2. Simulation Setup

2.1 Geometry and computational mesh

The computational model uses the modified NACA 0012 profile supplied by the NASA Turbulence Modeling Resource (TMR). The geometry is scaled to produce a sharp, closed trailing edge at x/c = 1. The chord is c = 1 m, the leading edge is at the origin and the x-axis follows the chord line.

The NASA TMR Family II, Level-4 structured C-grid contains 897 × 2 × 257 nodes, corresponding to 229,376 hexahedral cells. Its C-type topology wraps around the airfoil and reconnects in the wake. One cell is used in the spanwise y-direction, giving a quasi-two-dimensional domain, while z is the airfoil-normal direction. The farfield is approximately 500 chord lengths from the airfoil, and the airfoil surface contains 512 boundary faces.

2.2 Flow conditions and physical models

Steady, fully turbulent RANS calculations use the standard Spalart-Allmaras model. Air is treated as an ideal gas with $\gamma = 1.4$ and $R = 287.058\ \mathrm{J\ kg^{-1}\ K^{-1}}$. The freestream state is defined by:

$$a_\infty = \sqrt{(\gamma R T_\infty)}, \quad U_\infty = M_\infty a_\infty$$

$$Re_c = \rho_\infty U_\infty c / \mu_\infty, \quad p_\infty = \rho_\infty R T_\infty$$

Dynamic viscosity is evaluated using Sutherland's law:

$$\mu(T) = \mu_0 (T/T_0)^{3/2} [(T_0 + S)/(T + S)]$$

where $\mu_0 = 1.716 \times 10^{-5}$ Pa s, $T_0 = 273.15$ K and $S = 110.4$ K. Incidence is imposed in the x-z plane:

$$U_x = U_\infty \cos\alpha, \quad U_y = 0, \quad U_z = U_\infty \sin\alpha$$

The SA farfield condition is:

$$\tilde{\nu}_\infty/\nu_\infty = 3, \quad \mu_{t,\infty}/\mu_\infty = 0.210438$$

The airfoil is treated as an adiabatic no-slip wall with low-Reynolds-number near-wall integration and no wall function. Characteristic farfield conditions are applied to the outer boundaries, with symmetry conditions on the two spanwise planes.

2.3 Numerical method and convergence

The inviscid fluxes are evaluated using the SLAU2 scheme. Flow variables are reconstructed at cell faces using second-order MUSCL reconstruction with the van Albada limiter.

The convergence targets for the normalised mean-flow and SA residuals are:

$$\hat{R}_{NS} \le 10^{-12}, \quad \hat{R}_{SA} \le 10^{-10}$$

where $\hat{R}_{NS}$ and $\hat{R}_{SA}$ denote the normalised mean-flow and Spalart-Allmaras residuals.

Table 1. Simulation configuration for the NACA 0012 validation cases.

Category	Setting	Value or description
Geometry	Reference chord	$c = 1$ m
Mesh	Grid	NASA Family II, Level 4; structured C-grid
Mesh	Resolution	897 × 2 × 257 nodes; 229,376 hexahedral cells
Flow	Simulation type	Steady, fully turbulent compressible RANS
Flow	Mach number	$M_\infty = 0.15$
Flow	Chord Reynolds number	$Re_c = 6.0 \times 10^6$
Flow	Temperature	$T_\infty = 300$ K
Flow	Velocity	$U_\infty = 52.0836$ m s^{-1}
Flow	Density	$\rho_\infty = 2.12649$ kg m^{-3}
Flow	Dynamic viscosity	$\mu_\infty = 1.84592 \times 10^{-5}$ Pa s
Flow	Static pressure	$p_\infty = 1.83127 \times 10^5$ Pa
Flow	Angles of attack	$\alpha = 0°, 10°, 15°$
Material	Gas model	Ideal gas; $\gamma = 1.4$, $R = 287.058$ J kg^{-1} K^{-1}
Material	Viscosity model	Sutherland law
Turbulence	Model	Standard Spalart-Allmaras; low-Reynolds-number wall treatment
Turbulence	Farfield condition	$\tilde{\nu}_\infty/\nu_\infty = 3$; $\mu_{t,\infty}/\mu_\infty = 0.210438$
Boundary conditions	Airfoil	Adiabatic no-slip wall; no wall function
Boundary conditions	Outer boundary	Characteristic farfield
Boundary conditions	Spanwise planes	Symmetry
Spatial discretisation	Reconstruction	Second-order MUSCL with van Albada limiter

3. Results

Results are compared using the chordwise coordinate x/c and angle of attack (AoA), α. C_p is the pressure coefficient, C_f the skin-friction coefficient, C_L the lift coefficient and C_D the drag coefficient. The coefficients are nondimensionalised by the freestream dynamic pressure $q_\infty = \tfrac{1}{2}\rho_\infty U_\infty^2$:

$$C_p = (p - p_\infty) / (\tfrac{1}{2}\rho_\infty U_\infty^2)$$

$$C_f = \tau_w / (\tfrac{1}{2}\rho_\infty U_\infty^2)$$

$$C_L = L / (\tfrac{1}{2}\rho_\infty U_\infty^2 S_{ref}), \qquad C_D = D / (\tfrac{1}{2}\rho_\infty U_\infty^2 S_{ref})$$

3.1. Angle of Attack 0°

At α = 0°, symmetry requires zero lift. FluxCore predicts $C_L = 0$ and $C_D = 0.00808$, matching Flow360 and lying within the spread of the reference solvers in Table 2.

Table 2. Integrated C_D and C_L at α = 0°.

Code	α	C_D	C_L
CFL3D	0	0.00819	0
FUN3D	0	0.00812	0
NTS	0	0.00813	0
JOE	0	0.00812	0
SUMB	0	0.00813	0
TURNS	0	0.0083	0
CGNS	0	0.00817	0
OVERFLOW	0	0.00838	0
Flow360	0	0.00808	-8.648E-07
FluxCore	0	0.00808	0

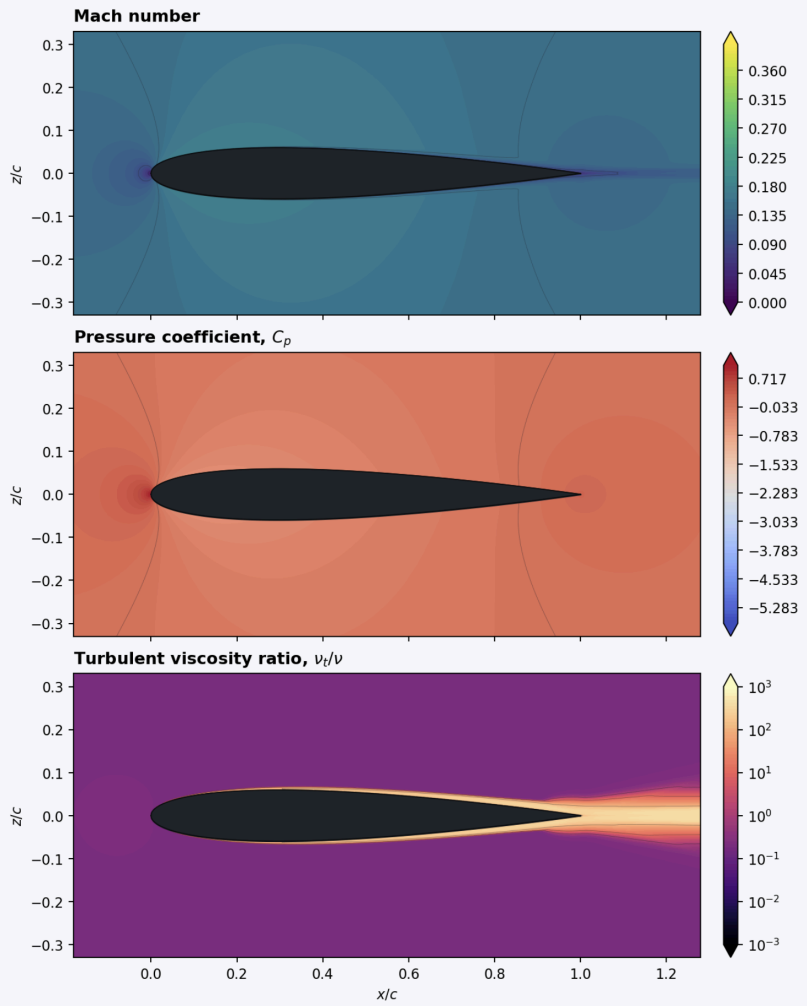


Figure 1. Mach number, pressure coefficient and turbulent-viscosity-ratio contours at α = 0°.

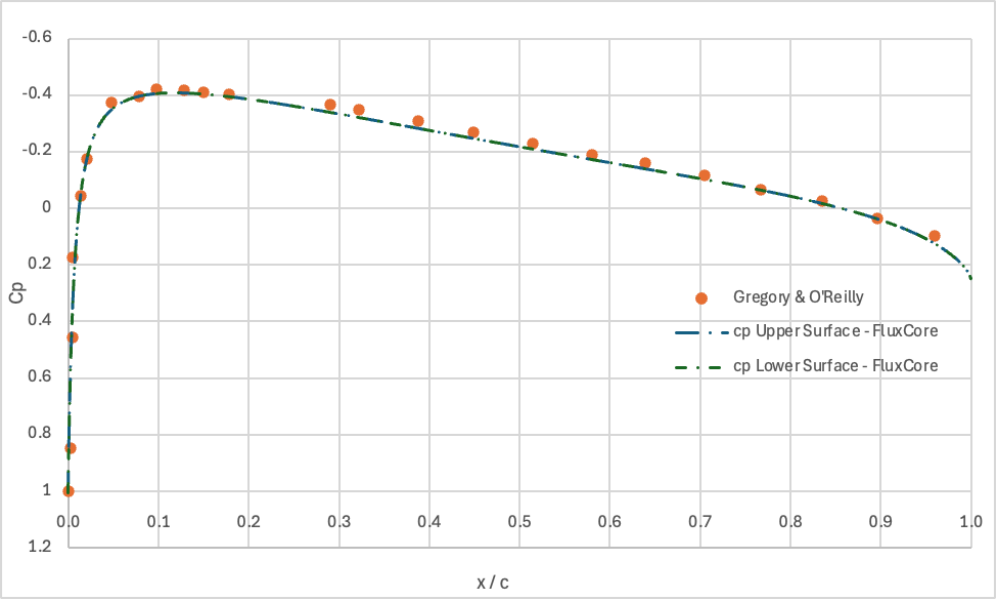


Figure 2. Surface pressure coefficient at α = 0°: FluxCore and Gregory and O'Reilly experimental measurements (Re_c = 2.88 × 10^6).

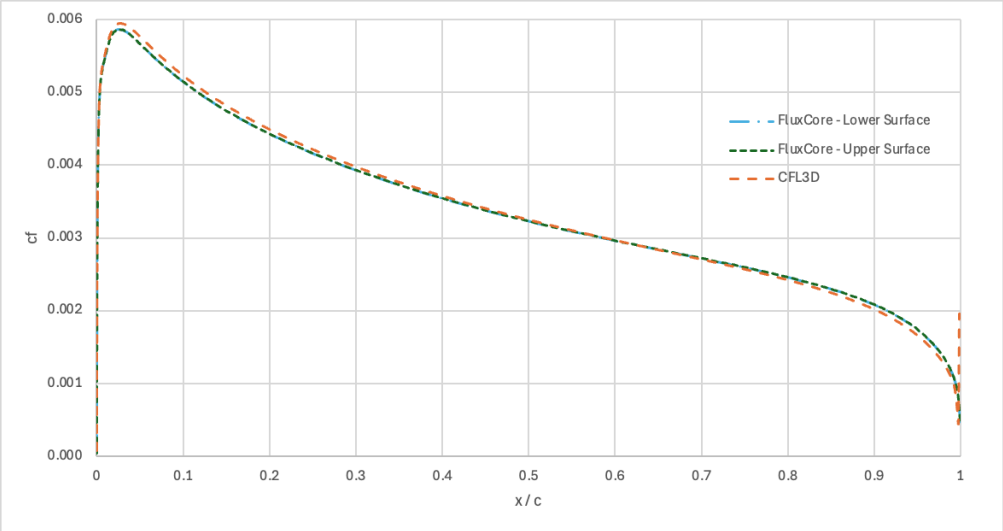


Figure 3. Surface skin-friction coefficient at α = 0°: FluxCore upper and lower surfaces and the CFL3D reference solution.

The flow-field contours and coincident upper- and lower-surface distributions confirm a symmetric attached solution. The computed pressure coefficient follows the Gregory and O'Reilly measurements over the chord, while C_f varies smoothly to the trailing edge.

3.2. Angle of Attack 10°

At α = 10°, FluxCore predicts C_L = 1.0893 and C_D = 0.01247. These values closely match the Flow360 results (1.0889 and 0.01244) and the wider reference set in Table 3.

Table 3. Integrated C_D and C_L at α = 10°.

Code	α	C_D	C_L
CFL3D	10	0.01231	1.0909
FUN3D	10	0.01242	1.0983
NTS	10	0.01243	1.0891
JOE	10	0.01245	1.0918
SUMB	10	0.01233	1.0904
TURNS	10	0.01230	1.1000
CGNS	10	0.01255	1.0941
OVERFLOW	10	0.01251	1.0990
Flow360	10	0.01244	1.0889
FluxCore	10	0.01247	1.0893

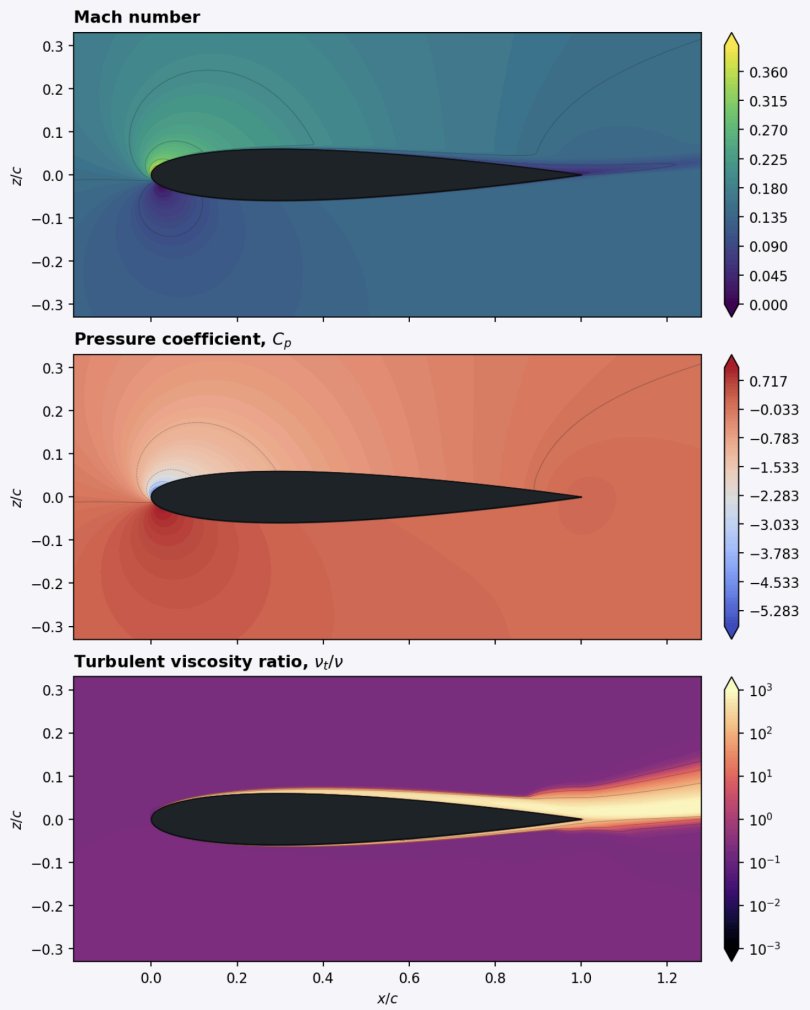


Figure 4. Mach number, pressure coefficient and turbulent-viscosity-ratio contours at α = 10°.

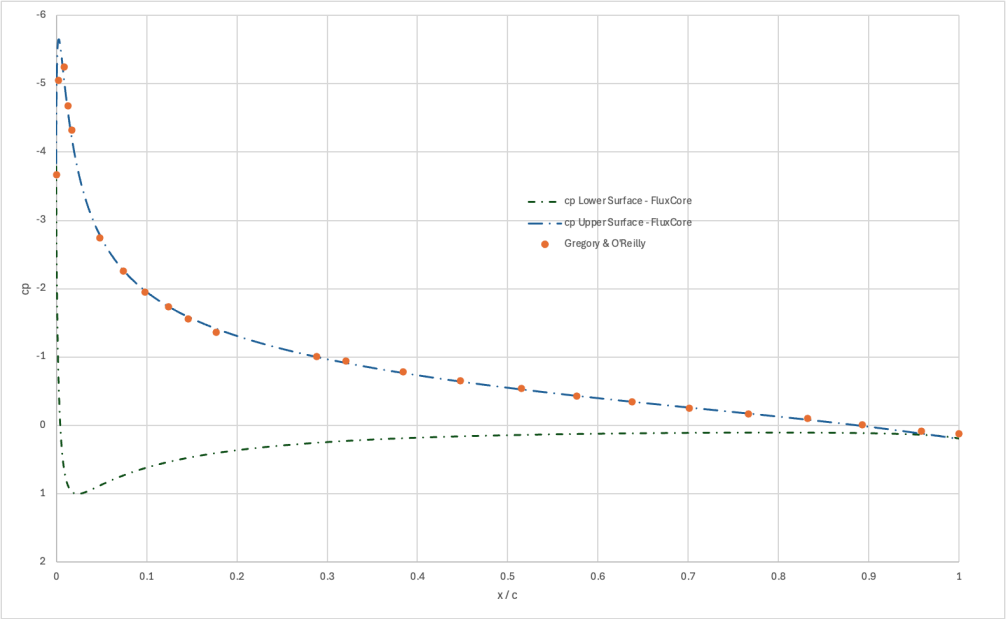


Figure 5. Surface pressure coefficient at α = 10°: FluxCore and Gregory and O'Reilly experimental measurements (Re_c = 2.88 × 10^6).

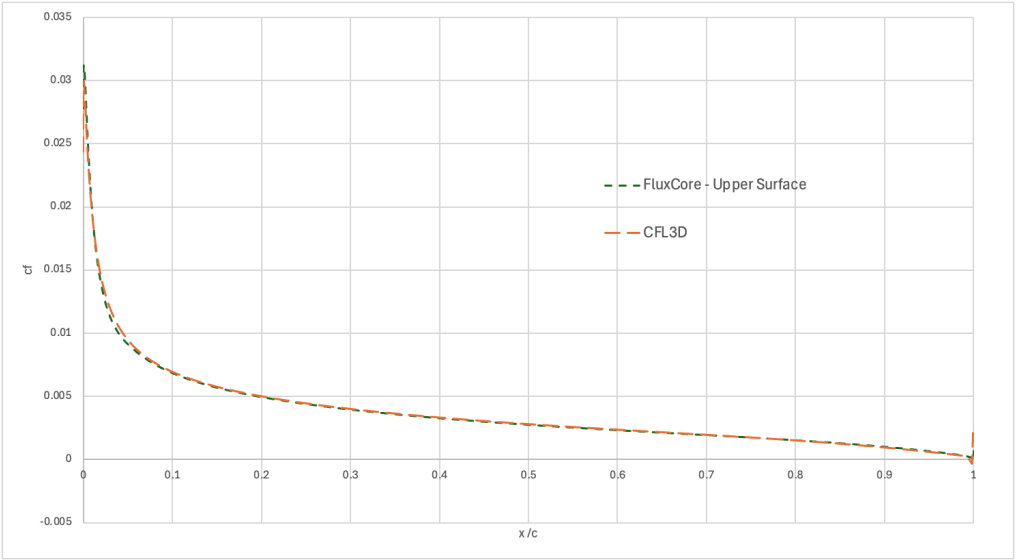


Figure 6. Surface skin-friction coefficient at α = 10°: FluxCore and the CFL3D reference solution.

The increased incidence produces a strong leading-edge suction peak and a thicker wake. FluxCore captures the measured pressure recovery, and the positive, smoothly decaying upper-surface C_f indicates that the mean flow remains attached.

3.3. Angle of Attack 15°

At α = 15°, FluxCore predicts C_L = 1.5451 and C_D = 0.02153. Both coefficients lie within the reference-solver range and differ from the Flow360 values by less than 0.5%.

Table 4. Integrated C_D and C_L at α = 15°.

Code	α	cd	cl
CFL3D	15	0.02124	1.5461
FUN3D	15	0.02159	1.5547
NTS	15	0.02105	1.5461
JOE	15	0.02148	1.5490
SUMB	15	0.02141	1.5546
TURNS	15	0.02140	1.5643
CGNS	15	0.02073	1.5576
OVERFLOW	15	0.02149	1.5576
Flow360	15	0.02158	1.5381
FluxCore	15	0.02153	1.5451

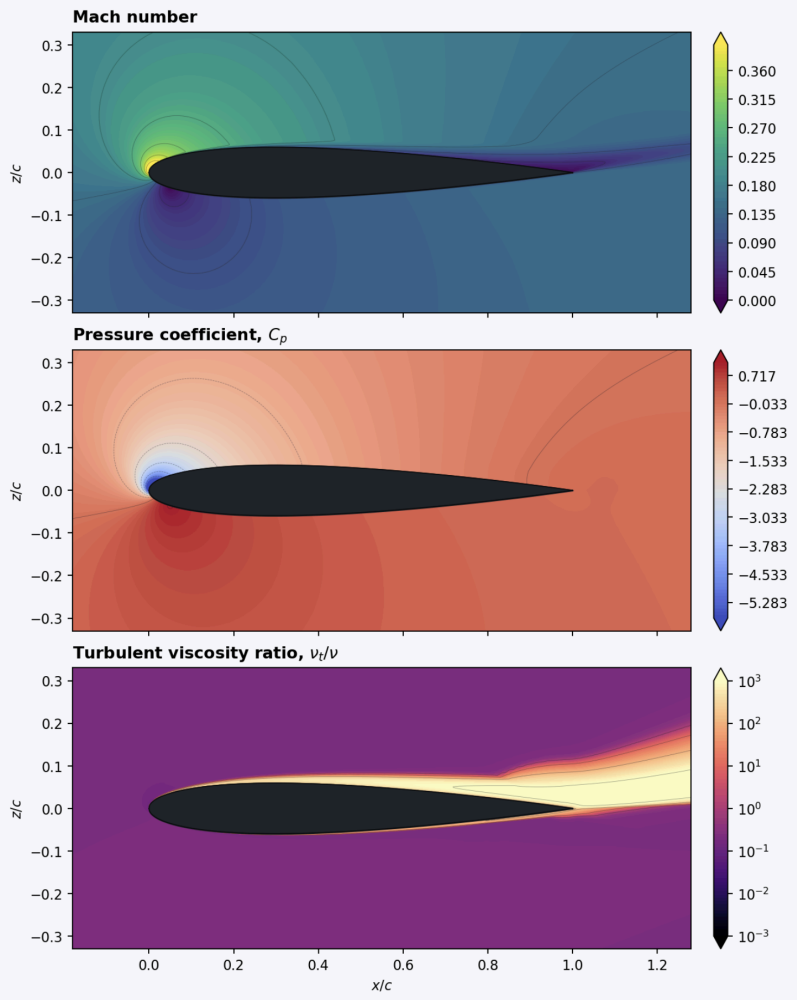


Figure 7. Mach number, pressure coefficient and turbulent-viscosity-ratio contours at α = 15°.

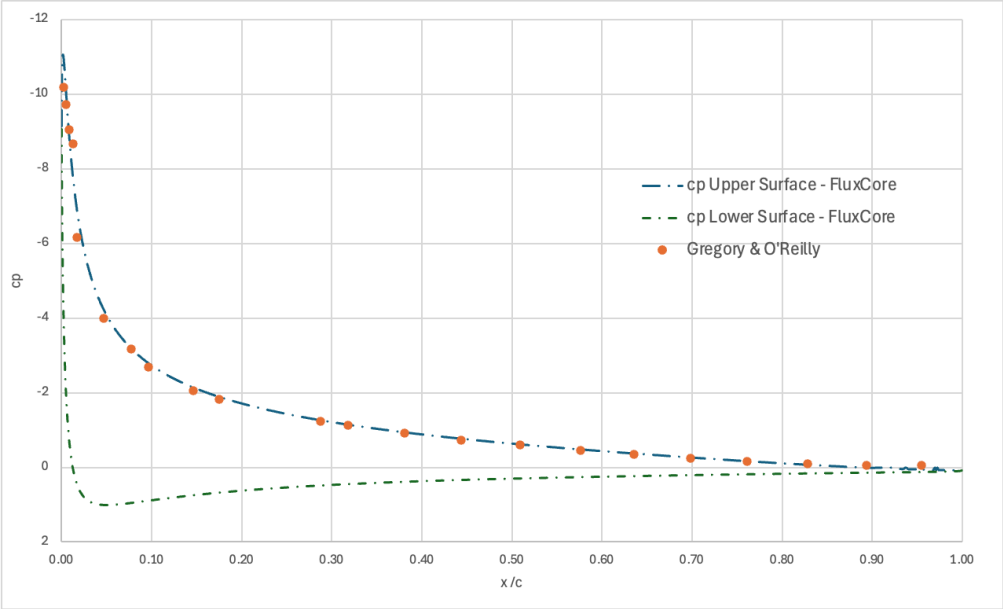


Figure 8. Surface pressure coefficient at α = 15°: FluxCore and Gregory and O'Reilly experimental measurements (Re_c = 2.88 × 10^6).

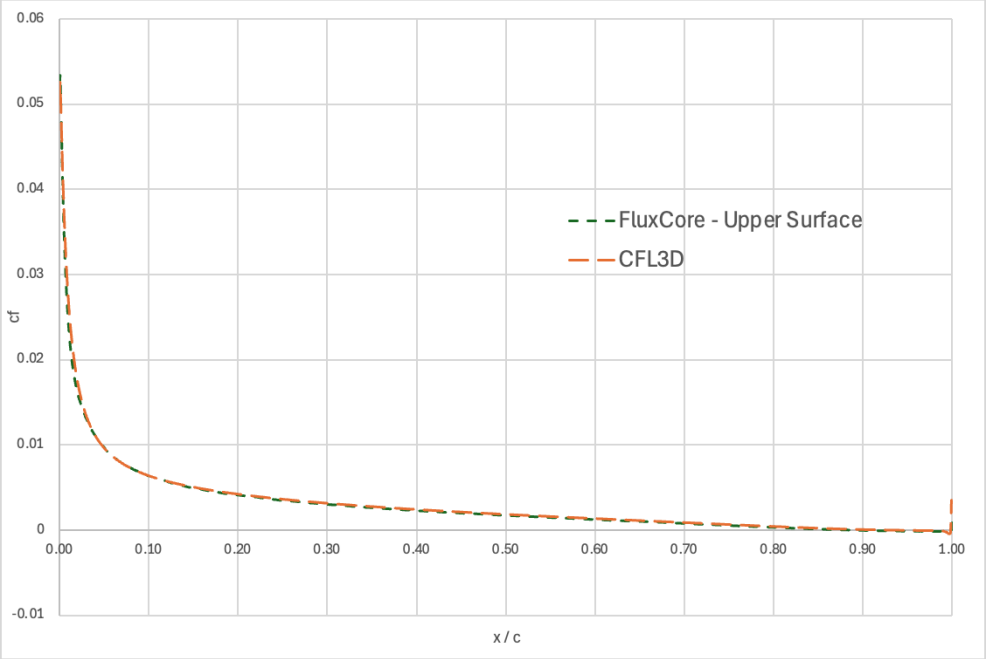


Figure 9. Upper-surface skin-friction coefficient at α = 15°: FluxCore and the CFL3D reference solution.

The suction-side pressure loading increases further at 15°. The upper-surface C_f falls towards zero near the trailing edge, consistent with incipient trailing-edge separation and the behaviour reported in the Flow360 and NASA TMR studies.

4. Summary

Across α = 0°, 10° and 15°, FluxCore reproduces the established NACA 0012 force-coefficient trends and remains within the spread of the reference CFD solutions. The surface C_p distributions

follow the Gregory and O'Reilly measurements, while the C_f results recover the expected progression from symmetric attached flow to incipient upper-surface separation at 15°. The lift curve also agrees closely with Ladson's tripped experimental data. Differences at high incidence should be interpreted in the context of experimental Reynolds-number differences and the increasing difficulty of maintaining two-dimensional flow near stall. Overall, the results support the implementation of the compressible RANS and standard SA model in FluxCore for this benchmark.

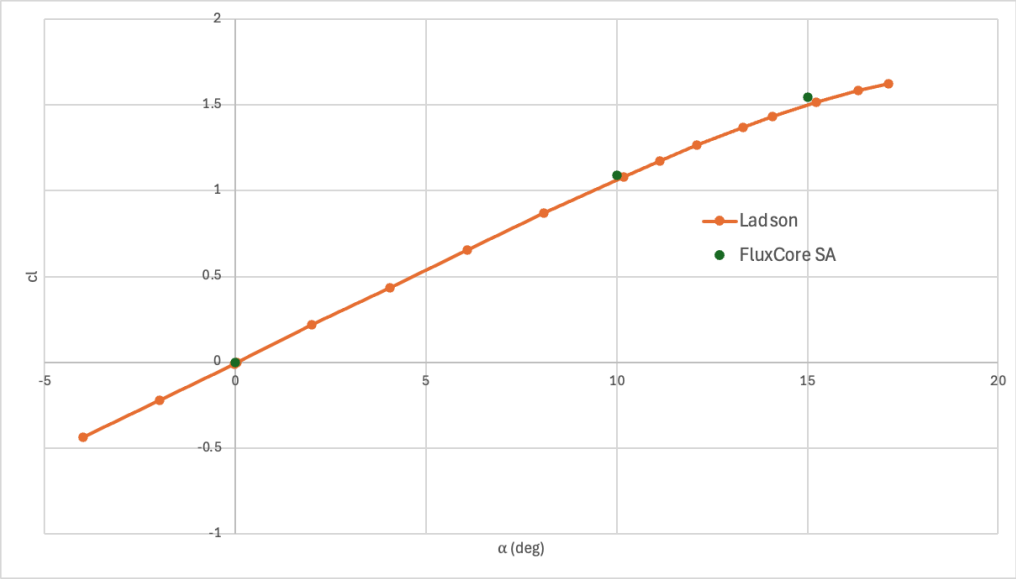


Figure 10. Lift coefficient versus angle of attack (AoA): FluxCore and the tripped experimental measurements of Ladson at Re_c = 6.0 × 10^6.

References

1. Flexcompute Inc. Flow360: NACA 0012 Low Speed Airfoil validation study.
2. NASA Langley Research Center. 2D NACA 0012 Airfoil Validation Case, Turbulence Modeling Resource (TMR).
3. Gregory, N. and O'Reilly, C. L. (1970). Low-Speed Aerodynamic Characteristics of NACA 0012 Aerofoil Section, including the Effects of Upper-Surface Roughness Simulating Hoar Frost. Reports and Memoranda No. 3726.
4. Ladson, C. L. (1988). Effects of Independent Variation of Mach and Reynolds Numbers on the Low-Speed Aerodynamic Characteristics of the NACA 0012 Airfoil Section. NASA TM-4074.